Effective single-band models for the high-T_c cuprates. II. Role of apical oxygen

R. Raimondi* and J. H. Jefferson
DRA Electronics Sector, St. Andrews Road, Great Malvern, Worcestershire WR14 3PS, England

L. F. Feiner
Philips Research Laboratories, Prof. Holstlaan 4, 5656 AA Eindhoven, The Netherlands
(Received 29 June 1995; revised manuscript received 21 November 1995)

An effective single-band model for the cuprates is derived by a cell-perturbation method from a five-band model which includes $d_{3z^2-r^2}$ orbitals on copper and p_z orbitals on apical oxygen. In addition to the usual Zhang-Rice singlets of A_1 symmetry, there are two-hole cell states of B_1 symmetry, which can become low in energy and depend sensitively on the apical oxygen ions. Provided that hybridization with the apical oxygen orbital is sufficiently weak to permit reduction to a t-t'-J model, the main effect of the B_1-symmetry states is to renormalize the effective next-nearest-neighbor hopping (t') of doped holes. This effect can be quite large and may even change the sign of t'. The variation of t' between various compounds due to differences in crystal structure is shown to correlate with $T_c^{\max}$, the critical temperature at optimum doping, suggesting that t' may be a crucial parameter for the low-energy physics, which moreover differentiates between the various cuprates. The effective single-band model is shown to break down when the apex level approaches the in-plane oxygen level, and to describe that situation, which cannot be ruled out completely for the cuprates with present experimental evidence, we propose a specific minimal effective (two-band) model.

I. INTRODUCTION

Extensive studies over the past five years have resulted in considerable evidence that the copper-oxide planes of the high-temperature superconductors may be modeled by an effective single-band model.[1,2] Nevertheless, this issue has remained controversial (see, e.g., the discussion in Refs. 1,2) because of arguments by Emery and Reiter[3] that the oxygen degrees of freedom are essential and would lead to a breakdown of an effective single-band description. In the preceding paper,[4] henceforth referred to as I, we have made a detailed investigation of the reduction of the three-band (d-p) model[5,6] to an effective single-band model for a wide range of parameters, using a cell-perturbation method. This leads to a single-band Hubbard model which differs from the usual form only in that effective hopping and Coulomb interactions between carriers are ''asymmetric.'' However, apart from these asymmetries and some small correction terms, the mapping of the three-band d-p model to an effective single-band Hubbard model is found to be extremely robust, with the effective parameters given very accurately in second order.

The validity of a single-band description of the cuprates has also been questioned from a quite different point of view. Various authors argued that the starting point, the three-band d-p model, is already insufficiently complete to capture all the relevant physics. In particular, calculations aiming at a realistic description of the electronic structure have indicated[7–10] that, in addition to the copper $3d_{x^2-y^2}$ and oxygen $2p_x$ and $2p_y$ σ orbitals included in the three-band model, the copper $3d_{3z^2-r^2}$ orbital may also be involved in accommodating doped holes. This has been confirmed by electron-energy-loss spectroscopy[11,12] and polarized x-ray-absorption spectroscopy,[13,14] although the occupancy is apparently considerably less than believed before.[15] In addition, various mechanisms for superconductivity have been proposed in which the $3d_{3z^2-r^2}$ orbital plays an essential role.[16–22] Further, there is experimental evidence that the out-of-plane (''apical'') oxygens affect the electronic structure in a way that is relevant to superconductivity. For example, in some compounds there is apparently a significant isotope effect for the apical oxygen,[23,24] and there is also a clear correlation between the maximum critical temperature $T_c^{\max}$ reached in different cuprates and the copper-apex bonding as estimated from the Cu bond valence sum.[25] Similarly, a correlation has been demonstrated between $T_c^{\max}$ and the Madelung potential at the apical oxygen relative to that at the planar oxygens.[26] One is thus led to take also the $2p_z$ orbital on the apical oxygen into account, and the basic model becomes the five-band d-p model considered in Refs. 27–29. It is clear that consideration of such an extended model, not entirely restricted to the Cu-O planes, is actually inevitable if one wants to account for the differences between the various cuprates.

In the present paper we therefore reconsider the reduction to a single-band model by the cell-perturbation method when the copper $3d_{3z^2-r^2}$ and apical oxygen p_z orbitals are included, thus starting from a five-band rather than a three-band model. As in previous investigations,[27–29] one particular aim of the present work is to possibly identify a characteristic quantity that is strongly affected by the apical oxygens (and thus differentiates between the various cuprates) and which can also be shown, at least empirically, to be related to high-T_c superconductivity. Our main result on this issue is that such a quantity actually exists within the single-band description, namely, that the *next-nearest-neighbor hopping parameter* t' in the t-t'-J model qualifies as the single parameter reflecting the main differences between the various cuprates.

The plan of the paper is as follows. In Sec. II we construct

the Hamiltonian for the five-band model in a cell basis, emphasizing the new aspects associated with the added orbitals, and referring for general information on the cell-perturbation method to paper I (where also further references can be found). This is followed in Sec. III by an examination of the most important effective hopping matrix elements and their variation with the energy of the apical p_z orbital and other d-p parameters. In Sec. IV we consider corrections to the usual effective single-band (t-t'-J) model caused by the extra orbitals and, particularly, the apical oxygen. This includes a critical discussion of the validity of the effective single-band model, speculating on when, and why, it might break down and what minimal model it could be replaced with. In Sec. V we discuss the significance of t' and examine the correlation between t' as calculated here and the experimental values of $T_c^{\max}$ for various cuprates. Finally, the main results are summarized and further discussed in Sec. VI.

II. EFFECTIVE HAMILTONIAN FOR THE FIVE-BAND MODEL

The usual three-band d-p model of the copper-oxide planes in the high-temperature superconductors is a tight-binding model with (hole) orbitals on copper ($3d_{x^2-y^2}\equiv d_x$) and oxygen ($2p_x$,$2p_y$) and includes Cu-O and O-O hopping interactions (t_{pd} and t_{pp}), on-site and nearest-neighbor Coulomb interactions (U_p, U_d, and V_{pd}), and on-site energies (ε_p and ε_d) [see Eq. (2.1) of I]. Estimates pertinent to the cuprates have converged (see I) towards a ''standard'' set of parameters (in units of $t_{pd}\approx 1.3$ eV) $\varepsilon\equiv\varepsilon_p-\varepsilon_d=2.7$, $t_{pd}=1$, $t_{pp}=0.5$, $U_d=7$, $U_p=3$, and $V_{pd}=1$, firmly putting the cuprates in the charge-transfer (rather than the Mott-Hubbard) regime in the Zaanen-Sawatzky-Allen diagram.[30] We now extend the three-band Hamiltonian by including the $3d_{3z^2-r^2}\equiv d_z$ orbital on copper and the $2p_z$ orbitals on apical oxygen. The localized energy of a hole in an apical p_z orbital we denote by $\varepsilon_{\rm apex}$ and that of a d_z hole by ε_z (representing a crystal-field splitting between d_z and d_x orbitals of $\varepsilon_z-\varepsilon_d$). Estimates for these parameters for the cuprates are (again in units of t_{pd}) $\varepsilon_z\lesssim 0.5$,[27,31] while $\varepsilon_{\rm apex}$ varies considerably from compound to compound because of the variation of Madelung potentials, ranging between 1.6 and 4.6.[27] Since the main aim of this paper is to investigate the effects of the extra (p_z,d_z) orbitals, and the results do not change in any significant way with the Coulomb parameters U_p and V_{pd} (provided the latter is not too large), then we set these to zero. Since this also decreases the effective gap (see I), we increase ε by about unity to compensate, when referring to the ''standard'' set.

In a preliminary step the in-plane oxygen orbitals are transformed into Wannier orbitals b and a, transforming locally like b_1 and a_1. In contrast to the three-band case the a orbitals must be retained because they hybridize strongly with the d_z and p_z orbitals. It is then important to exploit the freedom left in the definition of the Wannier orbitals by choosing a phase factor which ensures that *both* a_i *and* b_i are derived mainly from the four oxygen p_x and p_y orbitals surrounding the Cu site i. The first step in the cell approach is now to write the Hamiltonian of the five-band model in the (d_x,d_z,a,b,p_z) cell basis, and in the form $H=H_0+H_{\rm cc}$, where $H_0=\Sigma_i h_i$ describes noninteracting cells and $H_{\rm cc}$ is the cell-cell interaction. Because orbitals of different local symmetry do not hybridize within a cell, the single-cell Hamiltonian h can be split into three parts,

$$h=h^{(b_1)}+h^{(a_1)}+h^{(a_1b_1)}, \tag{2.1}$$

where

$$h^{(b_1)}=\varepsilon_b n^{(b)}+U_d n_\uparrow^{(d_x)} n_\downarrow^{(d_x)}-\tau_b\sum_\sigma\ (d_{x,\sigma}^\dagger b_\sigma+\text{H.c.}), \tag{2.2}$$

$$h^{(a_1)}=\varepsilon_a n^{(a)}+\varepsilon_z n^{(d_z)}+\varepsilon_{\rm apex} n^{(p_z)}+U_d n_\uparrow^{(d_z)} n_\downarrow^{(d_z)}-\tau_a\sum_\sigma\ (d_{z,\sigma}^\dagger a_\sigma+\text{H.c.})-\tau'_{pd}\sum_\sigma\ (d_{z,\sigma}^\dagger p_{z,\sigma}+\text{H.c.})-\tau'_{pp}\sum_\sigma\ (a_\sigma^\dagger p_{z,\sigma}+\text{H.c.}), \tag{2.3}$$

$$h^{(a_1b_1)}=U_d n^{(d_x)} n^{(d_z)}, \tag{2.4}$$

with $\varepsilon_b=\varepsilon_p-\varepsilon_d-2t_{pp}\nu_{00}=\varepsilon_p-\varepsilon_d-1.4536\,t_{pp}$, $\varepsilon_a=\varepsilon_p-\varepsilon_d+2t_{pp}\nu_{00}=\varepsilon_p-\varepsilon_d+1.4536\,t_{pp}$ (the effective charge-transfer energies of the b band and the a band, respectively), $\tau_b=2t_{pd}\mu_{00}=1.9162\,t_{pd}$, $\tau_a=2t_{pd}\lambda_{00}/\sqrt{3}=0.8612\,t_{pd}$, $\tau'_{pd}=2t'_{pd}/\sqrt{3}=1.1547\,t'_{pd}$, and $\tau'_{pp}=2t'_{pp}\lambda_{00}=1.4916\,t'_{pp}$. The convention for the primed hopping parameters t'_{pd} and t'_{pp} for hops involving the apical oxygen has been chosen such that they become equal to t_{pd} and t_{pp}, respectively, when the apical oxygen atom is at the same distance from the copper atom as the in-plane oxygen atoms.[29,32]

It is now useful to decompose also the cell-cell interaction (which is of purely hopping type since we have set $U_p=V_{pd}=0$) according to the local symmetry of the orbitals involved:

$$H_{\rm cc}=H_{\rm hop}^{(b_1)}+H_{\rm hop}^{(a_1)}+H_{\rm hop}^{(a_1b_1)}, \tag{2.5}$$

where

$$H_{\rm hop}^{(b_1)} = -2t_{pd}\sum_{i\neq j}\sum_{\sigma}\mu_{ij}(d^{\dagger}_{x,i\sigma}b_{j\sigma}+b^{\dagger}_{i\sigma}d_{x,j\sigma}) - 2t_{pp}\sum_{i\neq j}\sum_{\sigma}\nu_{ij}b^{\dagger}_{i\sigma}b_{j\sigma}, \tag{2.6}$$

$$H_{\rm hop}^{(a_1)} = -\frac{2}{\sqrt{3}}t_{pd}\sum_{i\neq j}\sum_{\sigma}\lambda_{ij}(d^{\dagger}_{z,i\sigma}a_{j\sigma}+a^{\dagger}_{i\sigma}d_{z,j\sigma}) + 2t_{pp}\sum_{i\neq j}\sum_{\sigma}\nu_{ij}a^{\dagger}_{i\sigma}a_{j\sigma} - 2t'_{pp}\sum_{i\neq j}\sum_{\sigma}\lambda_{ij}(p^{\dagger}_{z,i\sigma}a_{j\sigma}+a^{\dagger}_{i\sigma}p_{z,j\sigma}), \tag{2.7}$$

$$H_{\rm hop}^{(a_1b_1)} = +\frac{2}{\sqrt{3}}t_{pd}\sum_{i\neq j}\sum_{\sigma}\xi_{ij}(d^{\dagger}_{z,i\sigma}b_{j\sigma}+b^{\dagger}_{i\sigma}d_{z,j\sigma}) - 2t_{pp}\sum_{i\neq j}\sum_{\sigma}\chi_{ij}(a^{\dagger}_{i\sigma}b_{j\sigma}+b^{\dagger}_{i\sigma}a_{j\sigma}) + 2t'_{pp}\sum_{i\neq j}\sum_{\sigma}\xi_{ij}(p^{\dagger}_{z,i\sigma}b_{j\sigma}+b^{\dagger}_{i\sigma}p_{z,j\sigma}), \tag{2.8}$$

where the coefficients μ_{ij}, ν_{ij}, λ_{ij}, ξ_{ij}, and χ_{ij} follow from the Wannier transformation (see Appendix A). One should note that μ_{ij}, ν_{ij}, and λ_{ij}, describing hybridization between orbitals of the same symmetry, depend only on the distance between sites i and j. By contrast the coefficients ξ_{ij} and χ_{ij}, which describe the hybridization between a_1- and b_1-symmetry orbitals, also depend on the orientation of the vector $\mathbf{R}_{ij}$ connecting i and j: they change sign when $\mathbf{R}_{ij}$ is reflected in one of the [11] directions (and so in particular are zero for sites connected diagonally). This is of course due to the different *"nodality"* of a_1- and b_1-symmetry orbitals: a b_1 orbital changes sign under a 90° rotation while an a_1 orbital does not. It is further important to recognize that while hopping between in-plane oxygen orbitals of a_1 symmetry is equally efficient as between those of b_1 symmetry (involving the same coefficients ν_{ij}), holes in d_z and apical p_z orbitals are rather "immobile": direct hops between them ($d_z \leftrightarrow d_z$, $p_z \leftrightarrow p_z$, $d_z \leftrightarrow p_z$) are not permitted, and the nearest-neighbor hybridization hops in the a_1 channel are weaker by $\lambda_{01}/\sqrt{3}\mu_{01} < 1/\sqrt{3}$ and $t'_{pp}\lambda_{01}/t_{pd}\mu_{01} < t'_{pp}/t_{pd}$ (for $d_z \leftrightarrow a$ and $p_z \leftrightarrow a$, respectively) than those in the corresponding b_1 channel ($d_x \leftrightarrow b$).

The next and essential step of the cell method is to determine the eigenstates $|\nu\rangle$ of the single-cell Hamiltonian h [Eq. (2.1)], which can of course be done exactly, and subsequently express the full Hamiltonian in terms of these cell eigenstates. Using Hubbard's X operators[33] $X_i^{\nu'\nu} \equiv |i\nu'\rangle\langle i\nu|$, one obtains

$$H = \sum_i \sum_{\nu} E_{\nu} X_i^{\nu\nu} + \sum_{\langle ij\rangle} \sum_{\nu\nu'\mu\mu'} t_{ij}^{\nu'\nu\mu'\mu} X_i^{\nu'\nu} X_j^{\mu'\mu}, \tag{2.9}$$

where the second sum is over all pairs of sites (but not restricted to nearest neighbors). We emphasize that (2.9) is still entirely equivalent to the Hamiltonian in the (d_x, d_z, a, b, p_z) basis, and all intracell energies E_ν and cell-to-cell hopping parameters $t_{ij}^{\nu'\nu\mu'\mu} \equiv \langle i\nu', j\mu'|H_{\rm cc}|i\nu, j\mu\rangle$ can be calculated from the original parameters. Reduction to an effective single-band model is achieved by retaining in each cell only the zero-hole (full-shell, vacuum) state $|0\rangle$, the lowest-energy one-hole doublet $|g_\sigma\rangle$, and the lowest two-hole (singlet) cell state $|S\rangle$ (the generalized Zhang-Rice singlet[34,35]), and accounting for the effect of all the dropped cell states by second-order perturbation theory (see I). In the case of the three-band model, as usually considered, and after dropping the a orbitals, the number of cell states is rather limited. The inclusion of the extra orbitals, although straightforward, implies that the summations in (2.9) include many more cell states, reflecting the increased dimension of the Hilbert space, and one must reconsider whether reduction to an effective single-band model is still justified. Fortunately a considerable simplification can be achieved, both conceptually and practically, by making proper use of the symmetry of the cell states.

Let us consider first the main effect of the new hole orbitals, which transform locally like a_1, starting with the in-plane oxygen Wannier orbital a. This orbital lies at energy ε_a, about $3t_{pp}$ above the in-plane oxygen b orbital of b_1 symmetry at energy ε_b [see Eqs. (2.3) and (2.2)]. In the three-band model the a orbital provides the only *one-hole cell state* of a_1 symmetry. The energy of the lowest one-hole state of b_1 symmetry is then significantly lower due to hybridization between the b orbital and $3d_{x^2-y^2}$ on copper (via t_{pd}), even when ε_a and/or ε_b are small (see Fig. 1, and also Appendix B where the explicit form of the intracell Hamiltonian matrices is given). For the *two-hole states* we may construct states with local A_1 symmetry from two orbitals with b_1 symmetry, and states with local B_1 symmetry from a b_1 orbital and an a_1 orbital. In the three-band model the A_1 state splits into a lowest singlet [the Zhang-Rice (ZR) singlet[34] $|S\rangle$] and a triplet [the Emery-Reiter (ER) triplet[3] $|T_m\rangle$] at energy ε_b. This energy lowering of the singlet is again (and here *only*) due to hybridization via t_{pd} which cannot occur for the triplet due to the Pauli principle. The hybridization between the B_1 basis states $|d_x a\rangle$ and $|ba\rangle$, located at energies ε_a and $\varepsilon_a+\varepsilon_b$ respectively (see Fig. 1 and Appendix B), is weaker than between the A_1 singlet states $|d_x b\rangle_s = (|d_{x\uparrow} b_\downarrow\rangle - |d_{x\downarrow} b_\uparrow\rangle)/\sqrt{2}$ and $|b_\uparrow b_\downarrow\rangle$ because there is no mixing via the a orbital due to symmetry. The two-hole states of B_1 symmetry therefore lie considerably above the Zhang-Rice singlet.

Hence, since the local one- and two-hole states involving the a_1 orbitals are higher in energy than the lowest states involving only b_1 orbitals, the former are usually dropped and the three-band model is reduced to a two-band model, for the low-energy physics. This is, of course, an approximation for although the two manifolds of states are decoupled locally they can mix on neighboring cells [compare Eq. (2.8)], via effective hopping matrix elements. The importance of these (a_1-derived) states depends on the strength of the relevant hopping matrix elements and the difference in local energies in making such a transition, i.e., the ratio $|t/\Delta E|$. Upon reduction to an effective single-band model this therefore leads to corrections in perturbation

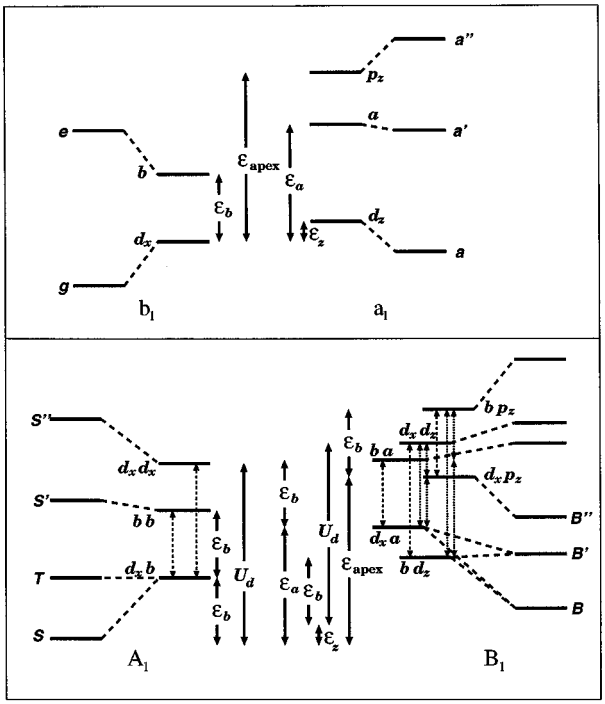

FIG. 1. Schematic energy level diagram of the cell states in the five-band model. Upper panel, one-hole states; lower panel, two-hole states. States in the three-band (Emery) model (b_1 and A_1) are shown on the left with additional states in the five-band model (a_1 and B_1) on the right. For the two-hole states hybridization in the b_1 (a_1) channel is indicated by dashed (dotted) arrows.

theory in exactly the same way as for the Emery-Reiter triplet (see I). Indeed, since the ER triplet and the lowest two-hole state with B_1 symmetry have comparable energies in the three-band model, there is no *a priori* reason to believe that the latter is any less important.

In the five-band model the potential significance of the a_1-derived states becomes greater since there is further energy lowering due to hybridization with the d_z orbitals on copper and the p_z orbitals on apical oxygen. In the *one-hole sector* the lowest state transforming like a_1 will now be dominated by its d_z component, at least as long as $\varepsilon_z < \varepsilon_a, \varepsilon_{\rm apex}$ (see Fig. 1). However, since the intracell hybridization between d_z and a is considerably weaker than between d_x and b [compare Eqs. (2.2) and (2.3)], the lowest b_1 one-hole state will then still be at significantly lower energy than the a_1 state. In the *two-hole sector* the presence of the d_z orbital will lead to a large $|bd_z\rangle$ component in at least one of the low-lying B_1 states (in the interesting regime of fairly large U_d the $|d_x d_z\rangle$ component will be relatively small). The other main component will be $|ga\rangle$, because the base states $|d_x a\rangle$ and $|ba\rangle$ hybridize, exactly like the one-hole base states $|d_x\rangle$ and $|b\rangle$, into a low-lying $|ga\rangle$ (and a high-lying $|ea\rangle$), thus gaining about $\tau_b^2/\varepsilon_b \approx 4t_{pd}^2/\varepsilon_b$ in energy. If $\varepsilon_z \lesssim \varepsilon_a - \varepsilon_b - 4t_{pd}^2/\varepsilon_b$, a condition well satisfied for the cuprates, it will be the lowest B_1-symmetry state (hereafter referred to as the B state) that is predominantly $|bd_z\rangle$ like, while the next-higher state $|B'\rangle$ will be mainly $|ga\rangle$, at least as long as $\varepsilon_{\rm apex}$ is sufficiently large (see again Fig. 1). One then expects the hybridization between $|bd_z\rangle$ and $|ba\rangle$ to push the B state significantly below the ER triplet.

The apical oxygen orbital p_z introduces the basis states $|d_x p_z\rangle$ and $|bp_z\rangle$ which hybridize among themselves into $|gp_z\rangle$ (and $|ep_z\rangle$) and subsequently mainly with $|ga\rangle$ and to a lesser extent with $|bd_z\rangle$. These new basis states thus influence the balance between the $|d_x a\rangle$ and $|bd_z\rangle$ components in the B state, and this in turn affects the magnitude of hopping matrix elements. Finally note that B_1 singlet and triplet states are degenerate as long as we ignore the Hund's-rule intraatomic exchange on copper, because all B_1 base states are necessarily constructed from two different orbitals, and so no triplet base states are excluded by the Pauli principle.

The behavior of the B_1-symmetry two-hole states described above is illustrated in Fig. 2(a) where we plot the energy of the six B_1 states (relative to the ZR singlet energy) versus the apex orbital energy. The energy of the ER triplet (dotted line) is also shown for comparison and appears, of course, as a horizontal line since it does not involve the apex orbital. In this figure we have used the ''standard'' parameter set for the cuprates and a realistic small value for the crystal-

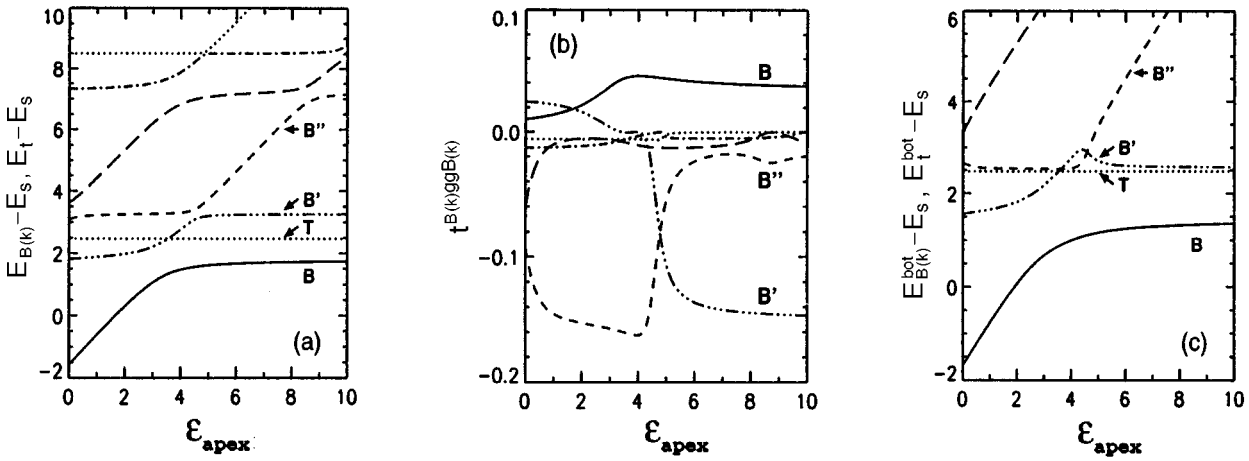

FIG. 2. (a) Cell state energies (relative to the ZR singlet energy), (b) hopping parameters, and (c) energies at the band bottom, of the six B_1-symmetry two-hole states, vs $\varepsilon_{\rm apex}$, with $t_{pd}=1.0$, $U_d=7$, $t_{pp}=0.5$, $t'_{pd}=0.5$, $t'_{pp}=0.25$, $\varepsilon_b=3$, $\varepsilon_z=0.5$.

field splitting, $\varepsilon_z = 0.5$, whereas for the hybridization of the apical oxygen p_z orbital we take $t'_{pd} = 0.5$ and $t'_{pp} = 0.25$, corresponding roughly to a copper-apex distance 20% larger than the in-plane oxygen copper distance.[27,29] (Here, as in the figures to follow, we have normalized to units of $t_{pd} = 1$.)

In Fig. 2(a) we note first that the B state is always lower in energy than the ER triplet, a feature emphasized for the cuprates by Eskes and Sawatzky.[10] This is not too surprising since the B state can profit more readily from hybridization without the restriction of the Pauli principle suffered by the ER triplet. Hence, to be consistent, if we are to calculate corrections to the effective single-band model due to the ER triplet, then we should, at least, also include corrections due to the B state. Since the latter involves the d_z orbitals on copper, then, even in the absence of the apicals, we would have to consider a four-band model. Fortunately, these corrections are quite small (but not insignificant as we show later) without the apicals and may be accounted for perturbatively. However, this is *not* the case when the apical is lowered in energy, as shown in the figure, when the B state becomes increasingly important and eventually even crosses the ZR singlet. We shall see in the next section that this may well be the situation for some of the cuprates.

Secondly we observe that the variation with $\varepsilon_{\text{apex}}$ can be simply understood as the state $|gp_z\rangle$ being "pulled through" the low-lying states $|B\rangle$ and $|B'\rangle$ when $\varepsilon_{\text{apex}}$ is lowered. The resulting anticrossings imply that when the apex level is high then $|B\rangle \approx |bd_z\rangle$ and $|B'\rangle \approx |ga\rangle$, while for small $\varepsilon_{\text{apex}}$ the B state finally becomes $|gp_z\rangle$, with $|B'\rangle \approx |bd_z\rangle$ and $|B''\rangle \approx |ga\rangle$. That this identification is correct may also be recognized from Fig. 2(b), which shows the nearest-neighbor hopping parameters $t^{B(k)ggB(k)}$ (where $k = 0,\ldots,5$), associated with the six B_1 two-hole states. They are defined as the amplitude for the process $|\ldots,g,B(k),\ldots\rangle \rightarrow |\ldots,B(k),g,\ldots\rangle$, and are a measure of the bandwidth of a propagating state $|B(k)\rangle$ in a background of doublets (spins) in the copper-oxide plane. The relatively large hopping parameter for the state $|B'\rangle$ at large $\varepsilon_{\text{apex}}$ corresponds to $|B'\rangle \approx |ga\rangle$ with the hole in the planar oxygen a orbital being fairly mobile, as pointed out above, and moving rather freely over the background of one-hole states (spins) $|g_\sigma\rangle$. Below the anticrossing at $\varepsilon_{\text{apex}} \approx 5$ that behavior is taken over by the state $|B''\rangle$. The hopping parameter of the B state remains much smaller throughout, being dominated by hops involving the rather "immobile" a_1-symmetry orbitals d_z and p_z at large and small $\varepsilon_{\text{apex}}$, respectively.

Validity of the reduction to an effective single-band model requires that upon hole doping only ZR singlets are created but no other two-hole states. Figure 2(a) already indicates that this condition might be not fulfilled at small $\varepsilon_{\text{apex}}$ because the B state could get occupied. It also suggests that the other B_1 states are sufficiently higher in energy and will remain unoccupied. However, whether occupation of a particular state occurs or not is of course determined by the energy at the bottom of the band that it gives rise to, while Fig. 2(a) shows cell energies which correspond to band centers. Since we have seen in Fig. 2(b) that the bandwidth of the B'- and B'' band can be rather large, one might wonder whether they would not get occupied more readily than the narrow B band. Figure 2(c) shows that this is not the case, simply because the relevant cell energies are too high. Here we have plotted the energy at the bottom of each of the B_1-symmetry bands,[36] $E^{\text{bot}}_{B(k)} = E_{B(k)} - 8|t^{B(k)ggB(k)}| + 8t'^{B(k)ggB(k)}$, where $t'^{B(k)ggB(k)}$ is the next-nearest-neighbor hopping parameter for state $|B(k)\rangle$.

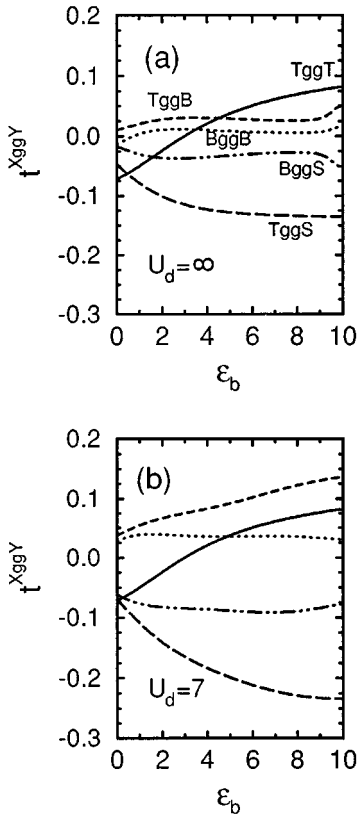

FIG. 3. Hopping and hybridization matrix elements involving the ZR singlet, ER triplet, and lowest state of B_1 symmetry showing dependence on U_d and ε_b, with $t_{pp} = 0.5$, $t'_{pd} = 0.5$, $t'_{pp} = 0.25$, $\varepsilon_z = 0$, and $\varepsilon_{\text{apex}} = 10$: t^{TggT} (solid line), t^{BggB} (dotted line), t^{TggB} (dashed line), t^{TggS} (long-dashed line), t^{BggS} (dot-dashed line). (a) $U_d = \infty$, (b) $U_d = 7$.

III. EFFECTIVE HOPPING TERMS

Having established that at most the B state could get physically occupied, it is of interest to study the behavior of that state in some more detail, and in particular compare with that of the ER triplet. We do so in Figs. 3–5, where we plot hopping matrix elements and local two-hole energies versus the relevant orbital energies.

In Fig. 3 we show the ε_b dependence of the five most important *nearest-neighbor* hopping matrix elements. Their meaning and significance is as follows. First, t^{TggT} represents the hopping of an Emery-Reiter triplet; i.e., it is the amplitude for the process $|\ldots,g,T,\ldots\rangle \rightarrow |\ldots,T,g\ldots\rangle$, just like t^{BggB} is the hopping matrix element for the B state. The remaining matrix elements t^{TggB}, t^{TggS}, and t^{BggS} again represent a two-hole hop but with a simultaneous transition to a different two-hole state, as indicated by the notation. They produce mixing between the various two-hole bands. In this figure we have set the crystal

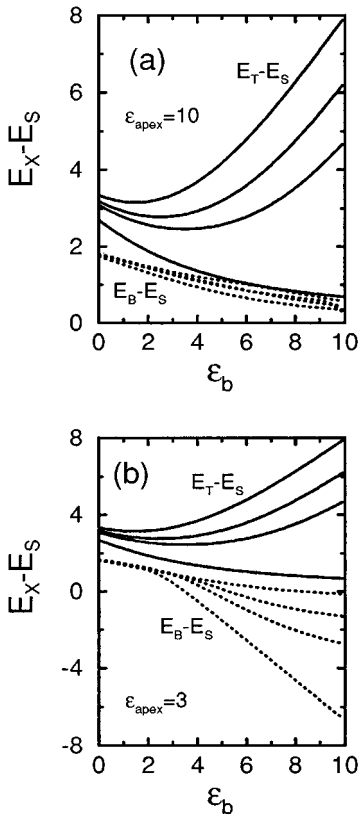

FIG. 4. Energy of the ER triplet relative to the ZR singlet (E_T-E_S, solid lines) and of lowest B_1 state (E_B-E_S, dotted lines), for $U_d=\infty$,7,5,3 (bottom to top curves). (a) $\varepsilon_{\text{apex}}=10$, (b) $\varepsilon_{\text{apex}}=3$. Other parameters as in Fig. 3.

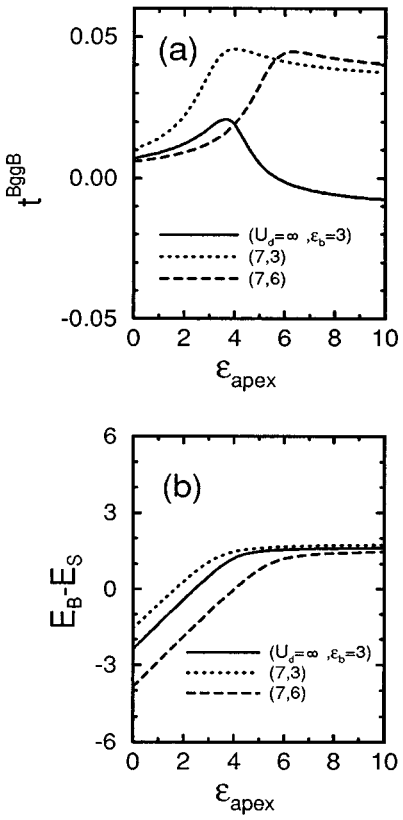

FIG. 5. (a) B state hopping matrix element t^{BggB}, (b) energy E_B-E_S, vs $\varepsilon_{\text{apex}}$, with $\varepsilon_z=0.5$ and $U_d=\infty$, $\varepsilon_b=3$ (solid line), $U_d=7$, $\varepsilon_b=3$ (dotted line), $U_d=7$,$\varepsilon_b=6$ (dashed line).

field splitting to zero ($\varepsilon_z=0$) and the energy of the apex level high ($\varepsilon_{\text{apex}}=10$). (Hence, except for large ε_b the apical oxygen has little effect.) We see from these plots that, in general, the bandwidth of the B state is less than that of the ER triplet. Indeed, t^{BggB} is smaller than the other matrix elements over the whole range of parameters. This is simply because the B state has significant admixtures of two-hole base states in which one hole is in a d_z orbital and this state is therefore rather immobile. (The d_z hole can only move when it is converted into an in-plane oxygen a hole. As pointed out in the previous section, the interaction for that process is weaker than that for converting a d_x hole into an in-plane b hole, which is the process involved in the corresponding motion of the Emery-Reiter triplet.) The other hopping matrix elements, i.e., t^{BggS}, t^{BggT}, and t^{TggS}, are broadly comparable in magnitude, which generally increases with ε_b. Note that these matrix elements have significantly greater magnitude for finite U_d compared with $U_d=\infty$, highlighting the importance of the states with two holes on copper. It is also noteworthy that t^{BggS} and t^{TggS} have a different variation with ε_b. One sees that t^{BggS} decreases slowly with ε_b, since for ε_b large, $|g_\sigma\rangle \approx |d_{x,\sigma}\rangle$ while $|S\rangle$ will primarily be composed of $|d_x b\rangle$ and $|d_{x,\uparrow} d_{x,\downarrow}\rangle$ and these can only be converted to $|B\rangle$ by the process $b \leftrightarrow a$, which is relatively weak. On the other hand, $|T\rangle$ and $|S\rangle$ tend to the same state (apart from spin) when ε_b becomes large, viz., $|d_x b\rangle$, for which there is an appreciable amplitude for hopping via $b \leftrightarrow b$ and $b \leftrightarrow d_x$.

Although the magnitude of t^{TggS} is greater than that of t^{BggS}, their relative importance with regard to corrections to the effective single-band model, or even the possibility of its breakdown, depends also on the energies E_B and E_T relative to that of the Zhang-Rice singlet E_S, as discussed in the previous section. We show these energies in Fig. 4(a) for the same parameters as in Fig. 3. We see again that over the whole parameter range the B state is lower than the ER triplet. In the present case of high apex orbital energy, these energies are an order of magnitude or more greater than the corresponding t's involved in the transition. We thus expect that they will lead to small perturbative corrections to the effective single-band model. This is indeed the case as we show later.

When the apex orbital is lowered in energy the situation can change significantly since the B state becomes much lower in energy. This is illustrated in Fig. 4(b) for which $\varepsilon_{\text{apex}}$ has been lowered to 3. With increasing ε_b the energy of the B state decreases with respect to that of the ZR singlet, and the B state actually crosses the ZR singlet for $\varepsilon_b \approx 5$, signaling a breakdown of the effective single-band model. If $\varepsilon_{\text{apex}}$ is reduced to 2, this crossover occurs already at $\varepsilon_b \approx 2$, which corresponds to an in-plane oxygen hole energy of 3.5 eV and an apical hole energy of 2.6 eV. Although there is some uncertainty in these parameters for the cuprates, they have been estimated for a range of materials and for some the apex-hole energies are indeed predicted to be close to or even below that of the in-plane oxygen holes, around 3 eV.[27] It thus appears that a breakdown of the effective single-band

model due to apical oxygen is a very real possibility in some materials.

There is a further interesting effect when we are close to this breakdown region (i.e., $E_B - E_S$ small), namely, that the effective bandwidth of the B state ($\sim|t^{BggB}|$) changes significantly in the region $\varepsilon_{\rm apex} \approx \varepsilon_b$, passing through a relatively pronounced maximum. This was already discernable in Fig. 2(b) and is shown in more detail in Fig. 5(a) where t^{BggB} is plotted against apex orbital energy. We see from Fig. 5(b), which shows the corresponding variation in $E_B - E_S$, that in each case this maximum in $|t^{BggB}|$ occurs in a region where $E_B - E_S$ is changing rapidly with apical hole energy, though still positive ($E_B - E_S \approx 1$ in all cases). For typical cuprate parameters (such as the dotted curve) the apical oxygen energies predicted for a number of materials are in the region of this peak.[27] Such an enhanced bandwidth is potentially significant if it concurs with a breakdown of the effective single-band model. In that situation there would be real hole occupation of the B band, which would then be expected to play a role in charge transport, in spite of $t^{BggB}_{\rm max}$ being considerably smaller than t^{SggS}, the nearest-neighbor hopping of ZR singlets. This is because the B state is spin independent (or at least nearly so when the Hund's rule intra-atomic splitting of the Cu d^8 configuration is included) and hence its motion is expected to be less inhibited by the spin background than the ZR singlets, which effectively become heavier due to a ''spin-string'' effect.[37]

The variation of t^{BggB} with the underlying parameters, $\varepsilon_{\rm apex}$, ε_b, ε_z, and U_d, can be understood as follows. First, consider the situation where the energy of the apex is so high that one deals essentially with the four-band model, and the B state is mainly a superposition of the in-plane base states $|bd_z\rangle$, $|d_x a\rangle$, $|ba\rangle$, and $|d_x d_z\rangle$. The hopping of the B state is then essentially controlled by the balance between the process $a \leftrightarrow a$ involving the two base states $|d_x a\rangle$ and $|ba\rangle$, and the process $d_z \leftrightarrow a$ involving also $|bd_z\rangle$ and to a lesser extent, depending upon the value of U_d, also $|d_x d_z\rangle$. Because the processes have opposite sign [see Eq. (2.7) and note that both λ_{01} and ν_{01} are <0], the net result depends sensitively on the participation of $|d_x d_z\rangle$ in the B state, i.e., on U_d [see Fig. 5(a)]. When $\varepsilon_{\rm apex}$ is decreased and the components $|d_x p_z\rangle$ and $|bp_z\rangle$ involving the apex orbital get mixed in, the hopping matrix element first increases because the process $p_z \leftrightarrow a$ involving these base states has the same sign as the $d_z \leftrightarrow a$ process [see again Eq. (2.7)]. Actually, the participation of the in-plane oxygen a orbital in the B state gets also increased slightly (compare Fig. 1) due to increased hybridization between $|d_x p_z\rangle$ and $|d_x a\rangle$ (and also between $|bp_z\rangle$ and $|ba\rangle$). Finally, however, when the energy of the apex orbital is lowered even further, the effect on the B bandwidth is rapidly reversed when $|d_x p_z\rangle$ becomes the dominant component in the B state approximately when $\varepsilon_{\rm apex} \lesssim \varepsilon_b$, as seen in Fig. 5(a). This is due to the decrease in d_z- and a-hole content, which frustrates the $d_z \leftrightarrow a$ and $p_z \leftrightarrow a$ processes, and the increase in (immobile) apex-hole content.

IV. EFFECTIVE SINGLE-BAND MODEL AND ITS POSSIBLE BREAKDOWN

As sketched in Sec. II and described in detail in I, the multi-band d-p model expressed in the cell basis may be reduced to a single-band model by simply restricting the Hilbert space to the lowest cell states, i.e., $|0\rangle$ (no holes), $|g_\sigma\rangle$ (one hole), and $|S\rangle$ (two holes, Zhang-Rice singlet). This immediately maps onto an asymmetric effective *single-band Hubbard model* with different effective hopping parameters for holes, $t^{hh}_{ij} = \langle iS, jg_\sigma | H_{\rm cc} | ig_\sigma, jS\rangle$, electrons, $t^{ee}_{ij} = \langle ig_\sigma, j0 | H_{\rm cc} | i0, jg_\sigma\rangle$, and interband transitions $t^{eh}_{ij} = \langle iS, j0 | H_{\rm cc} | ig_{\bar\sigma}, jg_\sigma\rangle$, and an effective Hubbard U given by $U_{\rm eff} = E_S + E_0 - 2E_g$ (of order ε_b in the charge-transfer regime, $U_d > \varepsilon_b$). When $U_{\rm eff} \gg t^{eh}$ this may then be further mapped onto a *charge-spin* (t-t'-J) *model*, describing either a hole-doped or an electron-doped system, where t and t' are the appropriate (hh or ee) nearest- and next-nearest-neighbor hopping parameters[38] and with $J = 4(t^{eh}_{01})^2 / U_{\rm eff}$.

We now discuss the main corrections to the effective single-band model produced by the a_1-symmetry orbitals, for the region of parameters where the single-band description is expected to remain valid. As in the reduction from the two-band model described in I, these corrections arise from higher-lying cell states and may be accounted for by perturbation theory provided that the levels involved are sufficiently high in energy. When reducing from the three-band or five-band model there are, of course, many more higher-lying cell states to be included in the summations over intermediate states. As stated above, the most important new state is the lowest two-hole state of B_1 symmetry (the B state). Provided it is not too low in energy, its main effect is to renormalize the *next-nearest-neighbor hopping* (t') in the effective single-band model. (It will also affect the nearest-neighbor hopping t and, for the charge-spin model, the superexchange J. However, for reasons of symmetry, these renormalizations are very small, as explained below.)

For the case of *hole doping* the second-order processes involved in this renormalization are of the form $|S,g,g\rangle \to |g,B,g\rangle \to |g,g,S\rangle$, i.e., the ZR singlet on cell 1 exchanges with a spin ($|\sigma\rangle \equiv |g_\sigma\rangle$) on cell 3 via an intermediate state involving the B state on cell 2. One must now distinguish the following cases: (i) for parallel spins: via the $m=0$ triplet component of the B state, $|S,\sigma,\sigma\rangle \to |\sigma, {}^3B_0, \sigma\rangle \to |\sigma,\sigma,S\rangle$, or via the singlet, $|S,\sigma,\sigma\rangle \to |\sigma, {}^1B_0, \sigma\rangle \to |\sigma,\sigma,S\rangle$; (ii) for antiparallel spins: via the $|m|=1$ triplet component, $|S,\bar\sigma,\sigma\rangle \to |\sigma, {}^3B_{2\bar\sigma}, \sigma\rangle \to |\sigma,\bar\sigma,S\rangle$; (iii) for antiparallel spins: via the $m=0$ triplet component, $|S,\bar\sigma,\sigma\rangle \to |\bar\sigma, {}^3B_0, \sigma\rangle \to |\bar\sigma,\sigma,S\rangle$, or via the singlet, $|S,\bar\sigma,\sigma\rangle \to |\bar\sigma, {}^1B_0, \sigma\rangle \to |\bar\sigma,\sigma,S\rangle$, with inversion of the spin on cell 2 and of the spin that exchanges with the ZR singlet. It is important to note that, as long as the intra-atomic Hund's-rule exchange on copper is neglected, actually no spin-flip processes are generated by the B state; i.e., the spin on cell 2 is the same in the final state as it was in the initial state. This is due to the degeneracy and identical orbital composition of singlet and triplet B states, so that $\langle {}^1B_0, \sigma | H_{\rm cc} | \sigma, S\rangle = \lambda_\sigma \langle {}^3B_0, \sigma | H_{\rm cc} | \sigma, S\rangle \equiv t^{BggS}$ (where $\lambda_\uparrow = 1$, $\lambda_\downarrow = -1$), which makes the spin-flipping sequences in (iii) exactly cancel one another. For the same reason the amplitude of the non-spin-flip process does not depend on the orientation of the spin on cell 2, because

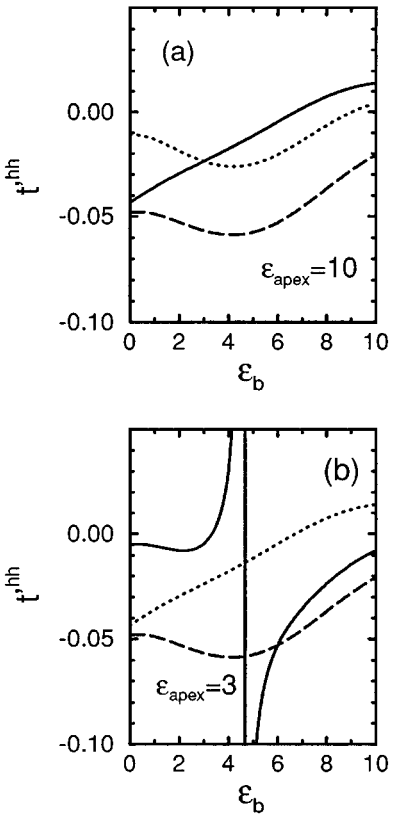

FIG. 6. Next-nearest-neighbor hopping for holes, t'^{hh}, vs ε_b, without (dotted line) and including the corrections due to the ER triplet (dashed line) and in addition that due to the B state (solid line), with $\varepsilon_z=0.5$. (a) $\varepsilon_{\text{apex}}=10$, (b) $\varepsilon_{\text{apex}}=3$.

$\langle {}^3B_{2\sigma},\bar{\sigma}|H_{\text{cc}}|\sigma,S\rangle=-\lambda_\sigma\sqrt{2}t^{BggS}$, so that the two processes (i) yield the same total correction for parallel spins as the single process (ii) does for antiparallel spins. Inclusion of the intra-atomic Hund's-rule exchange would obviously give rise to small deviations from this spin independence. Note further that as an immediate consequence of the (near) spin independence the contribution of second-order processes involving the B state to the superexchange J vanishes (or nearly so).

The resulting correction to t'^{hh} is therefore

$$\delta t'^{hh}(B)=+2\frac{2(t^{BggS})^2}{E_B-E_S}, \tag{4.1}$$

taking into account that there are two nearest-neighbor cells that can act as cell 2. Note that this second-order correction has *positive* sign because the two virtual hops $|S,g,g\rangle\rightarrow|g,B,g\rangle$ and $|g,B,g\rangle\rightarrow|g,g,S\rangle$ that make up the *effective diagonal* hop $|S,g\rangle\rightarrow|g,S\rangle$ are necessarily along different axes (one along x, one along y) and therefore contribute opposite signs. Referring to the discussion following Eq. (2.8) we emphasize that this important feature is due to the different *local symmetry* of a_1 and b_1 orbitals. [Similarly, the correction to nearest-neighbor hopping is almost zero because the expectedly dominant contributions involve one virtual (first-order) diagonal $b_1\leftrightarrow a_1$ hop, for which the matrix element vanishes by symmetry.] The effect of the B state on the next-nearest-neighbor hopping is shown in Fig. 6 where we plot t'^{hh} vs ε_b with and without the correction due to the B state. [Actually, the contributions from all B_1-symmetry two-hole states are included, but that from the (lowest) B state is dominant.] These plots also show the second-order correction due to the Emery-Reiter triplet (discussed in I and Ref. 39),

$$\delta t'^{hh}(T)=-2\frac{\frac{3}{2}(t^{TggS})^2}{E_T-E_S}. \tag{4.2}$$

In fact, the ER triplet gives a spin-dependent correction (as well as spin-flip terms) since cancellations like for the B state above do not occur, simply because there is no counterpart singlet to the ER triplet. In order to make a comparison with $\delta t'^{hh}(B)$ we have, in Eq. (4.2), taken the mean of spin-parallel and spin-antiparallel non-spin-flip corrections (which yields the factor 3/2), which corresponds physically to assuming that the ZR singlets move in a paramagnetic background; i.e., one-hole states have equal probability of having spin up or spin down. As seen in Fig. 6(a) (where $\varepsilon_{\text{apex}}=10$), when the apex orbital is high in energy the correction due to the B state is small, as expected (though comparable with that due to the ER triplet). Bringing down the apex level increases the correction due to the B state and with $\varepsilon_{\text{apex}}=3$ [Fig. 6(b)] its contribution is always greater than that of the ER triplet, or any other higher-lying state. Note that in this example the relative change in t'^{hh} becomes large for $\varepsilon_b\approx 3$ (the cuprates), since $\delta t'^{hh}(B)$ is then of the same order as t'^{hh}. The correction grows rapidly as ε_b is further increased to ≈ 4, eventually signaling a breakdown of the perturbation expansion and the mapping to an effective single-band model, as discussed above.

The sensitivity of t'^{hh} to the apex level is demonstrated more explicitly in Fig. 7 where we plot t'^{hh} vs $\varepsilon_{\text{apex}}$ for various U_d and ε_b, again with and without the B state contribution. We observe that there is a rapid suppression in the magnitude of t'^{hh} as the apex oxygen level is lowered in energy, in particular for finite U_d where the nearest-neighbor hopping parameter t^{BggS} is much larger than for $U_d=\infty$ (compare Fig. 3) as pointed out above. The plots further

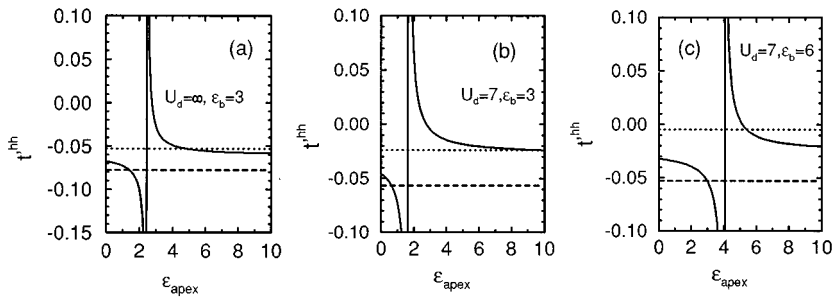

FIG. 7. Next-nearest-neighbor hopping for holes, t'^{hh}, vs $\varepsilon_{\text{apex}}$, without (dotted line) and including the corrections due to the ER triplet (dashed line) and in addition that due to the B state (solid line), with $\varepsilon_z=0.5$. (a) $U_d=\infty$, $\varepsilon_b=3$, (b) $U_d=7$, $\varepsilon_b=3$, (c) $U_d=7$, $\varepsilon_b=6$.

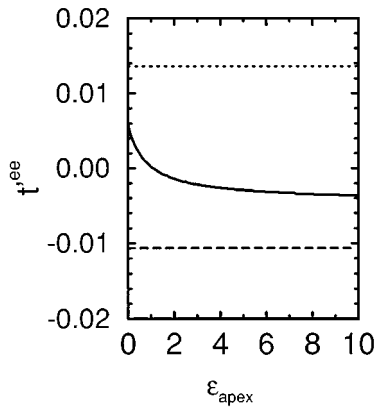

FIG. 8. Next-nearest-neighbor hopping for electrons, t'^{ee}, vs $\varepsilon_{\text{apex}}$, without (dotted line) and including the corrections due to the ER triplet (dashed line) and in addition that due to the B state (solid line), with $\varepsilon_z=0.5$, $U_d=7$, and $\varepsilon_b=3$.

show clearly that the region where the correction is large and the single-band description eventually breaks down is given roughly by $\varepsilon_{\text{apex}}\approx\varepsilon_b$. Note, however, that the formal breakdown always occurs for a value of $\varepsilon_{\text{apex}}$ that is smaller than ε_b, and significantly so for finite U_d. This is because it is determined by E_B-E_S becoming equal to zero, and both hybridization effects and the influence of U_d are stronger for the ZR singlet than for the B state [compare also Fig. 5(b)]. One should further note that for $\varepsilon_{\text{apex}}$ sufficiently low (but not so low as to cause breakdown) the correction due to the B states can even change the sign of t'^{hh}. So while t'^{hh} is generally negative in the three-band model (see I), this might not always be physically correct, since we see that it can become positive in the five-band model when the effect of the apicals is sufficiently strong.

It should be clear from the discussion above that similar second-order corrections are induced to the *third-neighbor hopping* t''^{hh} [i.e., from (0,0) to $(2a,0)$, etc.]. However, because the two virtual first-order hops are now in the same direction, the correction is *negative* here. Since there is further only one two-step path for this hopping process while there were two for the next-nearest-neighbor hop, $\delta t''^{hh}(B)=-\frac{1}{2}\delta t'^{hh}(B)<0$. The correction therefore adds to, instead of opposes, that from the ER triplet for which $\delta t''^{hh}(T)=+\frac{1}{2}\delta t'^{hh}(T)<0$. Third-neighbor and next-nearest-neighbor hopping parameters are actually comparable, and the present corrections are thus not insignificant.

In the case of *electron doping* the relevant processes are of the form $|0,g,g\rangle\rightarrow|0,B,0\rangle\rightarrow|g,g,0\rangle$. By the same argument as in the hole-doped case a net spin-independent hopping contribution results, and the correction to t'^{ee} is

$$\delta t'^{ee}(B)=+2\frac{2(t^{Bg0g})^2}{E_B+E_0-2E_g}, \tag{4.3}$$

again of *positive* sign. As the energy denominator here, which can be rewritten as $U_{\text{eff}}+E_B-E_S$, is always much larger than in the case of holes, the effective single-band model remains valid up to much smaller values of ε_b and $\varepsilon_{\text{apex}}$, and especially is not likely to break down in the parameter range of interest for the cuprates. Also the correction given by Eq. (4.3) remains fairly small, but it is not insignificant because the value for t'^{ee} resulting from the two-band model is small to begin with. This is demonstrated in Fig. 8, which shows the dependence of t'^{ee} on the apex orbital energy, with the same values for the other parameters as in the similar plots of t'^{hh} in Fig. 7(b). For this "standard" cuprate parameter set we find that the B state changes t'^{ee} from ≈-0.014 eV to ≈-0.003 eV. This confirms our finding in I that the next-nearest-neighbor hopping parameter is virtually zero for electron-doped cuprates. It also shows that when the effect of the apical oxygens is included, the sign of t'^{ee} will in general not change but remain negative. So, as long as $\varepsilon_{\text{apex}}$ is not too low, the signs of next-nearest-neighbor hole and electron hopping are still the same[40–42] (when the same sign convention is used for both; with the commonly used convention for the t-t'-J model the signs are then opposite[38]), but they may become opposite (and therefore equal with the t-t'-J model sign convention) when the apex level gets very low ($\varepsilon_{\text{apex}}\lesssim\varepsilon_b$) and the effect of the apicals changes the sign of t'^{hh} (see above).

With present uncertainties in the parameters for a multiband model, for the cuprates the possible breakdown of the mapping to an effective single-band model remains an open question, in particular for the more interesting case of hole doping. If it *does* break down, then a minimal model to describe the low-energy physics should contain the B state in the model subspace (i.e., the Hilbert space of the effective Hamiltonian). It is straightforward to do this in terms of Hubbard X operators by including terms involving the B states explicitly, just by retaining them in Eq. (2.9), resulting in an *effective two-band model*. Just like the effective single-band model can be expressed in terms of (effective) fermions $c^\dagger_{i\sigma}$, the inclusion of the B states may be represented simply as a new "band" of Fermi particles, created by $a^\dagger_{i\sigma}$. They are to be distinguished from the in-plane oxygen a orbitals, although the new "a" particles carry local a_1 symmetry and could be considered *effective* oxygen a holes. They hybridize with the "c" particles (which carry local b_1 symmetry). This description is correct provided we impose the constraints that a cell may only contain either a zero-hole state (no particles), a spin (one c particle), a ZR singlet (two c particles), or a B state (one c particle and one a particle). If we are in the regime where we can further reduce the effective two-band model to a charge-spin model, then we obtain for an *electron-doped system* just the usual t-t'-J model, but with corrections to the parameters due to the B state. However, for the *hole-doped case* we obtain the following two-band generalization of the t-t'-J model:

$$H^{(\text{two band})}_{tt'J}=P\left\{\sum_{ij\sigma}t^c_{ij}c^\dagger_{i\sigma}c_{j\sigma}+\sum_{\langle ij\rangle}\left[J\left(\mathbf{S}_i\cdot\mathbf{S}_j-\frac{1}{4}n_in_j\right)\right]+\sum_{ij\sigma}t^a_{ij}a^\dagger_{i\sigma}a_{j\sigma}+\sum_{ij\sigma}t^{ac}_{ij}(a^\dagger_{i\sigma}c_{j\sigma}+c^\dagger_{i\sigma}a_{j\sigma})+\epsilon_a\sum_i n^a_i\right\}P, \tag{4.4}$$

where $t_{ij}^{c}=t_{ij}^{SggS}$, $t_{ij}^{a}=t_{ij}^{BggB}$, $t_{ij}^{ac}=t_{ij}^{BggS}$, $\epsilon_a=E_B-E_S$, and P is now a projection operator which imposes the above constraints. Note that the convention used here is that both c and a are holes with respect to a "full shell" vacuum.

Over the last few years various two-band models have been proposed[43–45] based on the consideration that orbitals different from d_x and p_x/p_y, such as d_z and p_z, could be important. We emphasize that the model (4.4) proposed here is in fact *derived* in a straightforward way by the cell approach from the rather general five-band model, permitting its parameters to be calculated from the bare five-band parameters, for which rather reliable estimates are available, based upon the chemistry of the cuprates.[31,27]

V. ROLE OF t' AND CORRELATION WITH $T_c^{\max}$

We now discuss the possible significance of the suppression of t' for the hole-doped cuprates, and in particular its dependence on the coupling of the CuO_2 planes to the apical oxygens. We should first point out that the appreciable reduction of $|t'|$ due to the influence of the p_z orbital precisely in the cuprate regime [see Fig. 7(b)] is in good agreement with the results on band structure obtained by Grant and McMahan[31] in their Hartree-Fock plus configuration interaction calculations on clusters representing La_2CuO_4. They found that the dispersion along the line connecting $(\pi/2,\pi/2)$ to $(\pi,0)$ was strongly reduced by inclusion of apical p_z orbitals, and that their inclusion was absolutely essential for obtaining the weak dispersion observed experimentally.[46] This concurs therefore with the present finding, since we know that in the t-t'-J model the magnitude of that dispersion is largely governed by t', because the dispersion produced by t and J alone is very small because of correlation effects.[37,47–49] We therefore stipulate that the *next-nearest-neighbor hopping parameter* t' qualifies as the single parameter, which carries, *at the level of a single-band description*, the information about crystal structure outside the CuO_2 planes and thus *differentiates between the various cuprates.*

The role of t' in the t-t'-J model has received some further attention recently, after it had been realized that it is at least indispensable, as referred to above, for reproducing the flat quasiparticle dispersion and shape of the Fermi surface observed in the cuprates,[46] which in turn are held responsible for various (partly anomalous) normal-state properties.[50,51,48] Following early arguments by Lee[52] it has been conjectured that, although relatively small, t' may have a significant influence on the behavior of the model. In particular, Tohyama and Maekawa[53] have argued that the sign of t' is very important, this being a main distinguishing feature between electron-doped materials, for which t' is positive, and hole-doped materials for which t' is generally negative.[38] They showed by exact diagonalization on finite clusters that in the low-doping regime antiferromagnetic spin correlations are stabilized for $t'>0$, whereas a rapid destabilization takes place for $t'<0$. Further, it has since been shown by Gooding *et al.*[54] that both the spin distortions induced by doped carriers and the spatial distribution of the carriers are quite different for opposite t'. Obviously one would expect such differences in behavior to affect any tendency towards superconductive pairing quite strongly. Since we know that high-T_c superconductivity occurs much more readily and reaches much higher critical temperatures in hole-doped than in electron-doped cuprates, then apparently the sign of t' is crucial for superconductivity, negative t' being favorable, positive t' unfavorable. It is then tempting to speculate that also the *magnitude* of t' may have a decisive effect, resulting in a lower T_c as t' is made "more electron like," i.e., less negative for hole-doped systems.

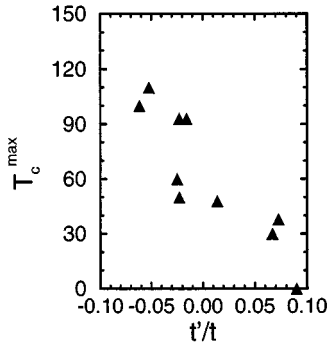

FIG. 9. Maximum critical temperature $T_c^{\max}$ vs t'/t for various superconducting cuprates. Compounds included are $La_2SrCu_2O_6$ ($T_c^{\max}=0$ K), $La_{1.85}Ba_{0.15}CuO_4$ ($T_c^{\max}=30$ K), $La_{1.85}Sr_{0.15}CuO_4$ ($T_c^{\max}=38$ K), $(Ba_{0.67}Eu_{0.33})_2$ $(Eu_{0.67}Ce_{0.33})_2\,Cu_3\,O_{8.78}$ ($T_c^{\max}=48$ K), $Y_{0.8}Ca_{0.2}Ba_2Cu_3O_{6.11}$ ($T_c^{\max}=50$ K), $YBa_2Cu_3O_{6.5}$ ($T_c^{\max}=60$ K), $YBa_2Cu_3O_7$ ($T_c^{\max}=93$ K), $Bi_2Sr_2Ca_{0.9}Y_{0.1}Cu_2O_{8.24}$ ($T_c^{\max}=93$ K), $TlBa_2CaCu_2O_7$ ($T_c^{\max}=100$ K), $Pb_{0.5}Tl_{0.5}Sr_2CaCu_2O_7$ ($T_c^{\max}=110$ K).

Since, as we have described above, the primary effect of apical oxygen on the parameters of the effective single-band model is to make a positive correction to t'^{hh} (mainly through the B state), then a stronger coupling of the apical oxygens to the CuO_2 planes (either due to a lower ϵ_{apex} or due to a larger t'_{pd} and t'_{pp} because of shorter copper-apex distance) should be detrimental to superconductivity if the aforementioned theoretical speculations are correct. There is experimental evidence that this is indeed the case, in particular the correlations between the critical temperature of various optimally doped materials on the one hand and the copper-apex bonding as estimated from the Cu bond valence sum[25] or the Madelung potential at the apical oxygen[26] on the other hand. Earlier theoretical work directly on the five-band model has been directed towards translating these empirical correlations into a correlation with quantities more directly related to the electronic structure of the CuO_2 planes, such as the stability of the ZR singlets [expressed by t (Ref. 27)] or the occupation of a_1-symmetry orbitals.[28,29] We may look similarly by the present approach for a correlation with the next-nearest-neighbor hopping by plotting for various materials the *experimentally observed* $T_c^{\max}$ (the maximum T_c, attained at the optimum doping value) versus the *calculated* t'/t. We have done so for the same ten representative cuprate compounds as in Refs. 28 and 29, with maximum critical temperatures ranging from 0 to 110 K, for which the parameters can be reliably computed from the data compiled in Ref. 27. The result is shown in Fig. 9, and we do indeed see the expected trend with $T_c^{\max}$ generally decreasing with increasing t'/t. We have verified that this result is robust by making similar plots for estimates of t_{pp} (and t'_{pp})

which are somewhat larger. While this gives quantitative differences, these are small, and the general trend is essentially the same. Clearly, the present finding is compatible with the general claims[52–54] about the importance of t', and in fact indicates that the *crystal structure* outside the CuO_2 planes *affects superconductivity via* t'.

The above result offers support for a scenario for high-T_c superconductivity based upon the t-t'-J model (or the Hubbard model with nearest and next-nearest-neighbor hopping) in which details of the quasiparticle dispersion of doped holes are quantitatively important. A noteworthy example would be the ''antiferromagnetic–Van Hove'' model, proposed recently by Dagotto, Nazarenko, and Moreo,[55] when properly extended to account explicitly for the effect of t'. In this model the antiferromagnetism of the cuprates is made responsible not only for the Van Hove singularity in the density of states (see below) but also for the pairing interaction. A second example would be the recent theory of d-wave superconductivity in the Hubbard model developed by Beenen and Edwards[56] and based upon Roth's procedure for decoupling Green's functions, again when extended to include t'.

To illustrate the point let us consider briefly the case of the t-t'-J model. It is by now well established[47–49] that the quasiparticle dispersion of a single hole doped into the half-filled antiferromagnetic insulator is then given accurately by

$$E(\mathbf{k}) = J[\alpha \cos k_x \cos k_y + \tfrac{1}{4}\beta(\cos 2k_x + \cos 2k_y)], \quad (5.1)$$

showing that the hole, which in our present picture has formed a ZR singlet, is forced to move within one magnetic sublattice in order not to disturb the antiferromagnetic spin background. On the assumption that this remains valid at finite doping one arrives at the picture where doped mobile spin-up (spin-down) holes move over the preexisting fixed spin-down (spin-up) holes that make up the magnetic sublattices. So doped holes of opposite spin remain spatially isolated and go into two distinct bands with identical dispersion given by Eq. (5.1). This has saddle points either at $S \equiv (\pm k_S, 0)$, $(0, \pm k_S)$ where $k_S = \pi - \arccos(\alpha/\beta)$, if $\beta > \alpha$, or at $(\pi/2, \pi/2)$ if $\beta < \alpha$, in either case producing a logarithmic Van Hove singularity in the density of states. In addition to the exact location of the saddle points also the flatness of the dispersion in their vicinity is determined by the ratio α/β. For the pure t-J model (i.e., for $t' = 0$) one has $\alpha \approx \beta \approx 1$ (see Refs. 47–49). Upon introduction of t' into the model α is replaced by $\alpha' = \alpha + 4t'/J$, while adding also t'' would similarly replace β by $\beta' = \beta + 8t''/J$. Then

$$\frac{\alpha'}{\beta'} \approx \frac{1 + 4t'/J}{1 + 8t''/J}, \quad (5.2)$$

and the location of the saddle points is seen to be largely determined by the *intrasublattice hopping parameter(s)* t' (and t'') rather than by t and/or J. The same holds for the flatness of the dispersion near the saddle points and thus for the width of the Van Hove singularity.

As for superconductivity it is clear that if this arises by any BCS-like pairing mechanism, then the critical temperature attained at optimum doping (as well as that doping value $\delta^{\max}$ itself) must depend now on α'/β', since quite generally $T_c^{\max}$ will be reached at the doping concentration that makes the Fermi surface pass through the saddle points. Consequently then $T_c^{\max}$ will depend critically on t' (and t'', if included), although the exact functional dependence, which may also depend on the form of the pairing interaction, is at present unknown and is currently the subject of further investigation. It is further clear that similar considerations must apply for the Beenen-Edwards treatment of superconductivity in the (t-t'-U) Hubbard model.[56]

So the following picture suggests itself. Frustrated motion of carriers, reflected in a very flat quasiparticle dispersion near the Fermi energy, is a prerequisite for the occurrence of high-T_c superconductivity. In the cuprates the frustration is due to the strong antiferromagnetic correlations of the background spins, and is governed, in a t-t'-J model description, by the effective *intersublattice* parameters t and J. These are characteristic for the *in-plane* chemistry and geometry of the CuO_2 planes and do not vary significantly between different cuprates. While the overall energy scale is now set by J, the actual value of $T_c^{\max}$ (and of $\delta^{\max}$) is, however, determined by the effective *intrasublattice* parameter(s) t' (and t''). For reasons of symmetry these depend mainly on the *out-of plane* chemistry and geometry, and can therefore have significantly different values for different cuprate compounds. Clearly, this scenario offers a plausible and simple explanation why $T_c^{\max}$ can vary so widely among the various cuprates, although there is hardly any variation in the geometry of the CuO_2 planes.

We should further point out that the effect of the apicals of reducing $|t'^{hh}|$ obtained here is perfectly compatible with their effect of enhancing the occupation of orbitals of a_1 symmetry found in Refs. 28,29. In those works it was shown in the context of a slave-boson mean-field correlated band-structure calculation (performed in the limit of an infinitely large U_d) that the apicals substantially increase the occupation of the in-plane oxygen a_1-symmetry orbitals while keeping their own occupation small. The corresponding effect in the present context of correlated bands derived from localized cell states is enhancing (by lowering the energy of the B state) the mixing between S and B bands. This can be viewed as the first-order admixture into a ZR singlet at a particular cell, of B states at nearest-neighbor cells, which accompanies the second-order correction $\delta t'^{hh}(B)$. Since the resulting effective ZR singlet then involves some a_1-symmetry orbitals, in particular the planar oxygen a orbital via the components $|d_x a\rangle$ and $|ba\rangle$, the occupation of those orbitals increases simultaneously with the decrease in $|t'^{hh}|$.

By contrast, in the present approach there is no reason to interpret this change in composition of the ZR singlet as a decrease of its stability, as put forward in Ref. 27; neither do we find any change in t induced by the apicals. It is only when the single-band model breaks down that one could say that the ZR singlets are no longer stable, in the sense that they do not suffice to describe all doped holes since one has in addition also real hole occupation of the B band. To describe such a situation one has to resort to a two-band model of the type given by (4.4). As discussed in Sec. III, then the B band is expected to play also a significant role in charge transport, since a B state can move without disturbing the spins, in contrast to a ZR singlet. In this context it is remark-

TABLE I. Wannier coefficients. Site i is the origin $0\equiv(0,0)$; site j is specified (in units of the Cu-Cu lattice parameter).

	$0\equiv(0,0)$	$1\equiv(1,0)$	$2\equiv(1,1)$	$3\equiv(2,0)$	$4\equiv(2,1)$	$5\equiv(2,2)$
μ	0.95809	−0.14009	−0.02351	−0.01373	−0.00685	−0.00327
ν	0.72676	−0.27324	0.12207	−0.06385	0.01737	0.01052
λ	0.74587	−0.17578	0.06179	−0.07134	0.01703	0.00925
ξ	0.00000	0.25763	0.00000	0.03913	0.00886	0.00000
χ	0.00000	0.13397	0.00000	−0.04056	0.03043	0.00000

able that $La_2SrCu_2O_6$, which does not become superconducting, is quite close to the breakdown regime. This suggests that high-T_c superconductivity disappears once the weakly correlated B band "short-circuits" the correlated ZR singlets, and that the single-band t-t'-J model is adequate to describe those cuprates that do superconduct, with the parameter t' differentiating between different compounds.

VI. SUMMARY AND CONCLUSIONS

In this paper we have shown that the effect of apical oxygen may be incorporated into a cell-perturbation scheme for reduction to an effective single-band model, by including p_z orbitals on apical oxygen and $d_{3z^2-r^2}$ orbitals on copper (five-band model). Provided the apical oxygen p_z orbital is not too low in energy the main effect is to *suppress next-nearest-neighbor hopping of doped holes* (i.e., Zhang-Rice singlets), having little effect on nearest-neighbor hopping and superexchange (for symmetry reasons) or on next-nearest-neighbor hopping of doped electrons. The effect is primarily due to a two-hole cell state of B_1 symmetry (the B state) being fairly low in energy compared to the ZR singlet. This leads to a rather large correction to t'^{hh}, associated with the virtual process by which a ZR singlet first makes a nearest-neighbor hop and changes into the two-hole B state followed by a further nearest-neighbor hop in an orthogonal direction, changing back again into a ZR singlet.

In the context of the t-t'-J model the reduction of $|t'|$ for hole-doped systems induced by the apical oxygens implies that the apicals strongly reduce the amplitude of the dispersion from $(\pi/2,\pi/2)$ to $(\pi,0)$, in agreement with numerical work[31] and with photoemission experiments.[46] We have argued that *at the level of the single-band description the influence of crystal structure*, in particular the differences between the various cuprates, *is fully reflected in the variation of* t'. Moreover, we have shown that the (detrimental) effect of the apical oxygens in hole-doped cuprates on high-T_c superconductivity translates into a correlation between t' and $T_c^{\max}$ (the maximum T_c at optimum doping). This supports recent results indicating the importance of t' for the behavior of the t-t'-J model,[53,54] and indicates that t' is also a crucial parameter for the strength of superconductive pairing. In particular our findings support scenarios, such as the recently proposed antiferromagnetic–Van Hove model[55] or the Beenen-Edwards theory of d-wave superconductivity in the Hubbard model,[56] where frustration of carrier motion is caused by the strong antiferromagnetism and is governed by t and J, which are basically in-plane parameters. We have argued that the actual value of $T_c^{\max}$ must then depend significantly on t', which would explain the variation of $T_c^{\max}$ between different compounds.

If the apical p_z-orbital energy becomes too low, then the effective single-band model eventually breaks down. This occurs when the B state gets close to, or even lower in energy than, the Zhang-Rice singlet, and it takes less energy to put a doped hole at the bottom of the B state-derived band than to create an extra ZR singlet. Such a situation cannot be accounted for perturbatively since there is "real" occupation of the B state. When this happens the B state also becomes more mobile (its bandwidth increases), due primarily to admixtures of base states involving holes on apical oxygen and in addition also in-plane oxygen holes of a_1 symmetry. Under such conditions the minimal model to describe the system is an effective two-band model containing doped holes whose motion is impeded by the spin background (the ZR singlets) and doped holes which are relatively unaffected by the spin background (the B states). We have also found evidence suggesting that superconductivity disappears when the single-band description becomes invalid. This picture is again consistent with the assertion that frustrated motion of carriers is essential for high-T_c superconductivity, and that such frustration is reduced by apical oxygen. Further study of the proposed two-band model would be of considerable interest, since it could shed more light on this issue.

Note added in proof. Further work[59] has since shown that when symmetry considerations are taken into account, it is more accurate to consider $t_- \equiv t' - 2t''$ rather than t' as the relevant parameter differentiating between the cuprates. This makes no difference for the physics and in particular does not change in any way our conclusions about the role of the apical oxygens and their effect on $T_c^{\max}$.

ACKNOWLEDGMENTS

We would like to thank C. Di Castro, H. Eskes, M. Grilli, and A.M. Oleś for stimulating discussions. This investigation was supported by the European Community under the SCIENCE program for collaborative research [Contract No. SC1*-0222-C(EDB)]. R.R. also acknowledges partial support by the European Union under Contract No. ERB 4050 PL 920925.

APPENDIX A: WANNIER TRANSFORMATION

The in-plane oxygen Wannier orbitals are defined by performing the following transformation in **k** space,

$$b_{\mathbf{k}\sigma}=i[s_x(\mathbf{k})p_{x,\mathbf{k}\sigma}-s_y(\mathbf{k})p_{y,\mathbf{k}\sigma}]/\sqrt{s_x^2(\mathbf{k})+s_y^2(\mathbf{k})}, \tag{A1}$$

$$a_{\mathbf{k}\sigma}=-i\,\mathrm{sgn}(k_xk_y)[s_y(\mathbf{k})p_{x,\mathbf{k}\sigma}+s_x(\mathbf{k})p_{y,\mathbf{k}\sigma}]/\sqrt{s_x^2(\mathbf{k})+s_y^2(\mathbf{k})}, \tag{A2}$$

where $s_x(\mathbf{k})=\sin(k_x/2)$ and $s_y(\mathbf{k})=\sin(k_y/2)$, and then Fourier transforming back to real space. The phase factor $\mathrm{sgn}(k_xk_y)$ in (1.2), added compared with Ref. 57, enhances the amplitude of $a_{i,\sigma}$ on the oxygen p orbitals closest to the Cu atom at site i.

The Wannier coefficients for hopping, μ_{ij}, ν_{ij}, λ_{ij}, ξ_{ij}, and χ_{ij}, resulting from this transformation are then obtained from

$$\mu(\mathbf{k})=\sqrt{s_x^2(\mathbf{k})+s_y^2(\mathbf{k})}, \tag{A3}$$

$$\nu(\mathbf{k})=4s_x^2(\mathbf{k})s_y^2(\mathbf{k})/\mu(\mathbf{k})^2, \tag{A4}$$

$$\lambda(\mathbf{k})=2|s_x(\mathbf{k})s_y(\mathbf{k})|/\mu(\mathbf{k}), \tag{A5}$$

$$\xi(\mathbf{k})=[s_x^2(\mathbf{k})-s_y^2(\mathbf{k})]/\mu(\mathbf{k}), \tag{A6}$$

$$\chi(\mathbf{k})=2|s_x(\mathbf{k})s_y(\mathbf{k})|[s_x^2(\mathbf{k})-s_y^2(\mathbf{k})]/\mu(\mathbf{k})^2, \tag{A7}$$

as the Fourier transform with respect to $\mathbf{R}_i-\mathbf{R}_j$. The values of these coefficients up to fifth neighbors are given in Table I.[58] Recall that ξ_{ij} and χ_{ij} change sign when $\mathbf{R}_i-\mathbf{R}_j$ is reflected in the [11] or $[\bar{1}1]$ direction, while μ_{ij}, ν_{ij}, and λ_{ij} are invariant under such a transformation. All coefficients are invariant under reflection in the x or y axis.

Similarly, the coefficients ϕ_{lij} and ψ_{klij}, relevant to the Coulomb interactions considered in I, are obtained from

$$\phi(\mathbf{k},\mathbf{k}')=2\frac{\cos[(k_x-k_x')/2]\sin(k_x/2)\sin(k_x'/2)+(x\rightarrow y)}{\mu(\mathbf{k})\mu(\mathbf{k}')}, \tag{A8}$$

$$\psi(\mathbf{k},\mathbf{k}',\mathbf{q})=\frac{s_x(\mathbf{k})s_x(\mathbf{k}+\mathbf{q})s_x(\mathbf{k}')s_x(\mathbf{k}'-\mathbf{q})+(x\rightarrow y)}{\mu(\mathbf{k})\mu(\mathbf{k}+\mathbf{q})\mu(\mathbf{k}')\mu(\mathbf{k}'-\mathbf{q})}, \tag{A9}$$

as the double Fourier transform with respect to $\mathbf{R}_i-\mathbf{R}_l$ and $\mathbf{R}_l-\mathbf{R}_j$ and the triple Fourier transform with respect to $\mathbf{R}_k-\mathbf{R}_l$, $\mathbf{R}_i-\mathbf{R}_j$, and $\mathbf{R}_j-\mathbf{R}_l$, respectively. Since $\phi(\mathbf{k},\mathbf{k})=2$ according to Eq. (A8), invoking the identity $(1/N)\Sigma_l e^{i(\mathbf{k}-\mathbf{k}')\cdot\mathbf{R}_l}=\delta_{\mathbf{k},\mathbf{k}'}$, we obtain the sum rule

$$\sum_l \phi_{lij}=\frac{1}{N}\sum_{\mathbf{k}} e^{i\mathbf{k}\cdot(\mathbf{R}_i-\mathbf{R}_j)}\phi(\mathbf{k},\mathbf{k})=2\,\delta_{ij}. \tag{A10}$$

A similar sum rule on the ψ_{llij} follows from Eq. (A9) according to

$$\begin{aligned}\sum_l \psi_{llij}&=\frac{1}{N^2}\sum_{\mathbf{k},\mathbf{k}'} e^{i\mathbf{k}'\cdot(\mathbf{R}_i-\mathbf{R}_j)}\psi(\mathbf{k},\mathbf{k}',\mathbf{0})\\&=\frac{1}{N^2}\sum_{\mathbf{k},\mathbf{k}'} e^{i\mathbf{k}'\cdot(\mathbf{R}_i-\mathbf{R}_j)}\frac{s_x^2(\mathbf{k})s_x^2(\mathbf{k}')+(x\rightarrow y)}{\mu(\mathbf{k})^2\mu(\mathbf{k}')^2}\\&=\frac{1}{2}\frac{1}{N}\sum_{\mathbf{k}'} e^{i\mathbf{k}'\cdot(\mathbf{R}_i-\mathbf{R}_j)}\frac{s_x^2(\mathbf{k}')+(x\rightarrow y)}{\mu(\mathbf{k}')^2}\\&=\frac{1}{2}\,\delta_{ij}.\end{aligned} \tag{A11}$$

APPENDIX B: INTRACELL HAMILTONIAN MATRICES

In the two-band model one has in each cell only the orbitals $d_{x,\sigma}$ and b_σ. The states in each n-hole sector are then determined by the following intracell Hamiltonian matrices (in the notation of I; to obtain them in the form relevant to the present paper, replace $\bar{\varepsilon}$ by ε_b and τ by τ_b, and in addition set $V_{db}=U_b=0$).

(0) Zero-hole states: $|0\rangle$, energy $E_0(=0)$.

(1) One-hole states: on the base states $|d_{x,\sigma}\rangle$ and $|b_\sigma\rangle$ the Hamiltonian is

$$h^{(1)}=\begin{pmatrix}0 & -\tau\\ -\tau & \bar{\varepsilon}\end{pmatrix}, \tag{B1}$$

yielding a ground-state doublet $|g_\sigma\rangle=\cos\theta|d_{x,\sigma}\rangle+\sin\theta|b_\sigma\rangle$ and an excited-state doublet $|e_\sigma\rangle=-\sin\theta|d_{x,\sigma}\rangle+\cos\theta|b_\sigma\rangle$, where $\tan2\theta=2\tau/\bar{\varepsilon}$, with energies $E_{g,e}=\bar{\varepsilon}/2\mp\sqrt{(\bar{\varepsilon}/2)^2+\tau^2}$.

(2|S) Two-hole states, singlet-sector: on the base states $|d_xb\rangle_S=(|d_{x,\uparrow}b_\downarrow\rangle-|d_{x,\downarrow}b_\uparrow\rangle)/\sqrt{2}$, $|b_\uparrow b_\downarrow\rangle$, and $|d_{x,\uparrow}d_{x,\downarrow}\rangle$ the Hamiltonian is

$$h^{(2|S)}=\begin{pmatrix}\bar{\varepsilon}+V_{db} & -\tau\sqrt{2} & -\tau\sqrt{2}\\ -\tau\sqrt{2} & 2\bar{\varepsilon}+U_b & 0\\ -\tau\sqrt{2} & 0 & U_d\end{pmatrix}, \tag{B2}$$

yielding eigenstates $|S\rangle$ (the generalized Zhang-Rice singlet), $|S'\rangle$, and $|S''\rangle$.

$(2|T)$ Two-hole states, triplet-sector: The base states $|d_{x,\uparrow}b_{\uparrow}\rangle$, $(|d_{x,\uparrow}b_{\downarrow}\rangle+|d_{x,\downarrow}b_{\uparrow}\rangle)/\sqrt{2}$, and $|d_{x,\downarrow}b_{\downarrow}\rangle$ are the components of the Emery-Reiter triplet $|T_m\rangle$, with energy $E_T=\bar{\varepsilon}+V_{db}$.

In the five-band model one has in addition the orbitals $d_{z,\sigma}$, a_{σ}, and $p_{z,\sigma}$. Now the following additional subspaces arise.

$(1|a_1)$ One-hole states (a_1 symmetry): on the base states $|d_{z,\sigma}\rangle$, $|a_{\sigma}\rangle$, and $|p_{z,\sigma}\rangle$ the Hamiltonian is

$$h^{(1|a_1)}=\begin{pmatrix} \varepsilon_z & -\tau_a & -\tau'_{pd} \\ -\tau_a & \varepsilon_a & -\tau'_{pp} \\ -\tau'_{pd} & -\tau'_{pp} & \varepsilon_{\text{apex}} \end{pmatrix}. \tag{B3}$$

$(2|B_1)$ Two-hole states (B_1 symmetry), singlet and triplet sectors: on the base states $|d_{x,\sigma}a_{\sigma'}\rangle$, $|b_{\sigma}a_{\sigma'}\rangle$, $|d_{x,\sigma}d_{z,\sigma'}\rangle$, $|b_{\sigma}d_{z,\sigma'}\rangle$, $|d_{x,\sigma}p_{z,\sigma'}\rangle$, and $|b_{\sigma}p_{z,\sigma'}\rangle$ the Hamiltonian is

$$h^{(2|B_1)}=\begin{pmatrix} \varepsilon_a & -\tau_b & -\tau_a & 0 & -\tau'_{pp} & 0 \\ -\tau_b & \varepsilon_b+\varepsilon_a & 0 & -\tau_a & 0 & -\tau'_{pp} \\ -\tau_a & 0 & \varepsilon_z+U_d & -\tau_b & -\tau'_{pd} & 0 \\ 0 & -\tau_a & -\tau_b & \varepsilon_b+\varepsilon_z & 0 & -\tau'_{pd} \\ -\tau'_{pp} & 0 & -\tau'_{pd} & 0 & \varepsilon_{\text{apex}} & -\tau_b \\ 0 & -\tau'_{pp} & 0 & -\tau'_{pd} & -\tau_b & \varepsilon_b+\varepsilon_{\text{apex}} \end{pmatrix}. \tag{B4}$$

*Present address: School of Physics and Chemistry, Lancaster University, Lancaster LA1 4YB, England.

[1] E. Dagotto, Rev. Mod. Phys. **66**, 763 (1994).

[2] W. Brenig, Phys. Rep. **251**, 153 (1995).

[3] V.J. Emery and G. Reiter, Phys. Rev. B **38**, 11938 (1988).

[4] L.F. Feiner, J.H. Jefferson, and R. Raimondi, preceding paper, Phys. Rev. B **53**, 8751 (1996).

[5] V.J. Emery, Phys. Rev. Lett. **58**, 2794 (1987).

[6] C.M. Varma, S. Schmitt-Rink, and E. Abrahams, Solid State Commun. **62**, 681 (1987).

[7] A. Fujimori, Phys. Rev. B **39**, 793 (1989).

[8] J.F. Annett, R.M. Martin, A.K. McMahan, and S. Satpathy, Phys. Rev. B **40**, 2620 (1989).

[9] J.B. Grant and A.K. McMahan, Phys. Rev. Lett. **66**, 488 (1991).

[10] H. Eskes and G.A. Sawatzky, Phys. Rev. B **44**, 9656 (1991).

[11] N. Nücker, H. Romberg, X.X. Xi, J. Fink, B. Gegenheimer, and Z.X. Zhao, Phys. Rev. B. **39**, 6619 (1989).

[12] H. Romberg, N. Nücker, M. Alexander, J. Fink, D. Hahn, T. Zetterer, H.H. Otto, and K.F. Renk, Phys. Rev. B **41**, 2609 (1990).

[13] C.T. Chen, L.H. Tjeng, J. Kwo, H.L. Kao, P. Rudolf, F. Sette, and R.M. Fleming, Phys. Rev. Lett. **68**, 2543 (1992).

[14] M. Pompa, P. Castrucci, C. Li, D. Udron, A.-M. Lagarde, H. Katayama-Yoshida, S. Della Longa, and A. Bianconi, Physica C **184**, 102 (1991).

[15] A. Bianconi, M. De Santis, A. Di Cicco, A.M. Flank, A. Fontaine, P. Lagarde, H. Katayama-Yoshida, and A. Kotani, Phys. Rev. B **38**, 7196 (1988).

[16] H. Kamimura, S. Matsuno, and R. Saito, Solid State Commun. **67**, 363 (1988).

[17] H. Kamimura, Int. J. Mod. Phys. B **1**, 699 (1988).

[18] Y.B. Gaidedey and V.M. Loktev, Phys. Status Solidi B **147**, 307 (1987).

[19] W. Weber, Z. Phys. B **70**, 323 (1988).

[20] D.L. Cox, M. Jarrell, C. Jayaprakash, H.R. Krishna-murthy, and J. Deisz, Phys. Rev. Lett. **62**, 2188 (1989).

[21] B.G. Vekhter, Chem. Phys. Lett. **176**, 67 (1991).

[22] D.I. Khomskiĭ and E.I. Neimark, Physica C **173**, 342 (1991).

[23] K.A. Müller, Z. Phys. B **80**, 193 (1990).

[24] J.H. Nickel, D.E. Morris, and J.W. Ager III, Phys. Rev. Lett. **70**, 81 (1993).

[25] D.M. de Leeuw, W.A. Groen, L.F. Feiner, and E.E. Havinga, Physica C **166**, 133 (1990).

[26] Y. Ohta, T. Tohyama, and S. Maekawa, Physica C **166**, 385 (1990).

[27] Y. Ohta, T. Tohyama, and S. Maekawa, Phys. Rev. B **43**, 2968 (1991).

[28] C. Di Castro, L.F. Feiner, and M. Grilli, Phys. Rev. Lett. **66**, 3209 (1991).

[29] L.F. Feiner, M. Grilli, and C. Di Castro, Phys. Rev. B **45**, 10 647 (1992).

[30] J. Zaanen, G.A. Sawatzky, and J.W. Allen, Phys. Rev. Lett. **55**, 418 (1985).

[31] J.B. Grant and A.K. McMahan, Phys. Rev. B **46**, 8440 (1992).

[32] The cases of one or two apical oxygen ions can be considered on equal footing: in the case of two (above and below the Cu-O planes) apical oxygens, a single bonding combination of $2p_z$ orbitals hybridizes with the plane, whereas a nonbonding combination can be factorized out. For this reason the Hamiltonians for one or two apical oxygen(s) only differ by a $\sqrt{2}$ normalization factor which rescales the plane-apical ions hopping integrals; Eqs. (2.3), (2.7), (2.8) correspond to the case of one apical oxygen ion.

[33] J. Hubbard, Proc. R. Soc. London A **277**, 237 (1964).

[34] F.C. Zhang and T.M. Rice, Phys. Rev. B **37**, 3757 (1988).

[35] H. Eskes and G.A. Sawatzky, Phys. Rev. Lett. **61**, 1415 (1988).

[36] The hopping parameters $t^{B(k)ggB(k)}$ are defined for the singlet component. In the absence of singlet-triplet splitting of the B_1 states the effective hopping parameter for a quasiparticle of definite spin direction is then $2t^{B(k)ggB(k)}$.

[37] S. Trugman, Phys. Rev. B **37**, 1597 (1988).

[38] With the usual convention for the t-J model of forbidding double occupancy, i.e., describing particles in a less than half-filled band and the coefficients of the hopping terms in the Hamiltonian being written as $-t$, $-t'$, etc., then $t=+t^{hh}$ ($t=-t^{ee}$) for a hole-doped (electron-doped) system. Here the sign convention for both t^{hh} and t^{ee} is that for holes, which we continue to use whenever we make explicit reference to the type of particles by means of superscripts. This cannot change the physics of course, but it is important that the relative sign of t' is correct.
[39] M.E. Simón and A.A. Aligia, Phys. Rev. B **52**, 7701 (1995).
[40] H. Eskes, G.A. Sawatzky, and L.F. Feiner, Physica C **160**, 424 (1989).
[41] M.S. Hybertsen, E.B. Stechel, M. Schlüter, and D.R. Jennison, Phys. Rev. B **41**, 11068 (1990).
[42] T. Tohyama and S. Maekawa, J. Phys. Soc. Jpn. **59**, 1760 (1990).
[43] H. Kamimura and M. Eto, J. Phys. Soc. Jpn. **59**, 3053 (1990).
[44] J. Zaanen, A.M. Oleś, and P. Horsch, Phys. Rev. B **46**, 5798 (1992).
[45] J. Ashkenazy, J. Supercond. **7**, 719 (1994); **8**, 559 (1995).
[46] D.S. Dessau, Z.-X. Shen, D.M. King, D.S. Marshall, L.W. Lombardo, P.H. Dickinson, A.G. Loeser, J. DiCarlo, A. Kapitulnik, and W.E. Spicer, Phys. Rev. Lett. **71**, 2781 (1993).
[47] K.J. von Szczepanski, P. Horsch, W.H. Stephan, and M. Ziegler, Phys. Rev. B **41**, 2017 (1990).
[48] E. Dagotto, A. Nazarenko, and M. Boninsegni, Phys. Rev. Lett. **73**, 728 (1994).
[49] J. Bala, A.M. Oleś, and J. Zaanen, J. Magn. Magn. Mater. **140-144**, 1939 (1995); Phys. Rev. B **52**, 4597 (1995).
[50] P. Bénard, L. Chen, and A.-M.S. Tremblay, Phys. Rev. B **47**, 15217 (1993).
[51] Q. Si, Y. Zha, K. Levin, and J P. Lu, Phys. Rev. B **47**, 9055 (1993).
[52] P.A. Lee, Phys. Rev. Lett. **63**, 680 (1989).
[53] T. Tohyama and S. Maekawa, Phys. Rev. B **49**, 3596 (1994).
[54] R.J. Gooding, K.J.E. Vos, and P.W. Leung, Phys. Rev. B **50**, 12 866 (1994).
[55] E. Dagotto, A. Nazarenko, and A. Moreo, Phys. Rev. Lett. **74**, 310 (1995).
[56] J. Beenen and D.M. Edwards, Phys. Rev. B **52**, 13 636 (1995).
[57] B.S. Shastry, Phys. Rev. Lett. **63**, 1288 (1989).
[58] These expansion coefficients are for an infinite plane. Equivalent coefficients for a finite system with periodic boundary conditions are calculated in the same way using Fourier summations. The differences are considerable and indicate that significant finite-size effects occur in finite-cluster studies of the five-band model.
[59] L. F. Feiner, J. H. Jefferson, and R. Raimondi (unpublished).